

Understanding the unstable convergence of gradient descent

Kwangjun Ahn*
 MIT EECS
kjahn@mit.edu

Jingzhao Zhang
 Tsinghua, IIIS
jzhzhang@mit.edu

Suvrit Sra
 MIT EECS
suvrit@mit.edu

Abstract

Most existing analyses of (stochastic) gradient descent rely on the condition that for L -smooth cost, the step size is less than $2/L$. However, many works have observed that in machine learning applications step sizes often do not fulfill this condition, yet (stochastic) gradient descent converges, albeit in an unstable manner. We investigate this unstable convergence phenomenon from first principles, and elucidate key causes behind it. We also identify its main characteristics, and how they interrelate, offering a transparent view backed by both theory and experiments.

1 Introduction

Gradient descent (GD) runs the iteration

$$\boldsymbol{\theta}^{t+1} = \boldsymbol{\theta}^t - \eta \nabla f(\boldsymbol{\theta}^t),$$

seeking to optimize a cost function f . It also provides a conceptual foundation for stochastic gradient descent (SGD), one of the key algorithms in modern machine learning. A vast body of literature that analyzes (S)GD assumes that the cost f is L -smooth (i.e., $\|\nabla f(\boldsymbol{\theta}^{t+1}) - \nabla f(\boldsymbol{\theta}^t)\| \leq L\|\boldsymbol{\theta}^{t+1} - \boldsymbol{\theta}^t\|$; for $f \in C^2$, equivalently $\|\nabla^2 f(\boldsymbol{\theta})\|_2^2 \leq L$), and subsequently exploits the associated “*descent lemma*”:

$$f(\boldsymbol{\theta}^{t+1}) \leq f(\boldsymbol{\theta}^t) - \eta \left(1 - L \frac{\eta}{2}\right) \|\nabla f(\boldsymbol{\theta}^t)\|^2. \quad (1)$$

To ensure descent via inequality (1), the condition

$$L < \frac{2}{\eta}, \quad (2)$$

is imposed. This condition ensure that GD decreases the cost f at each iteration. Whenever condition (2) holds, we call it the **stable regime** in this paper.

When the cost is quadratic, condition (2) is in fact necessary for stability: if $\eta > \frac{2}{L}$, then GD diverges (see Fact 1). This observation carries over to most convex optimization settings and also neural networks when using the neural tangent kernel approximation [Jacot et al., 2018, Lee et al., 2019, Li and Liang, 2018]. Thus, it is reasonable to assume condition (2) for those analyses. However, for general nonconvex costs, it is not clear whether the stable regime condition (2) is required or even reasonable.

*Part of this work was done while Kwangjun Ahn was visiting the Simons Institute for the Theory of Computing.

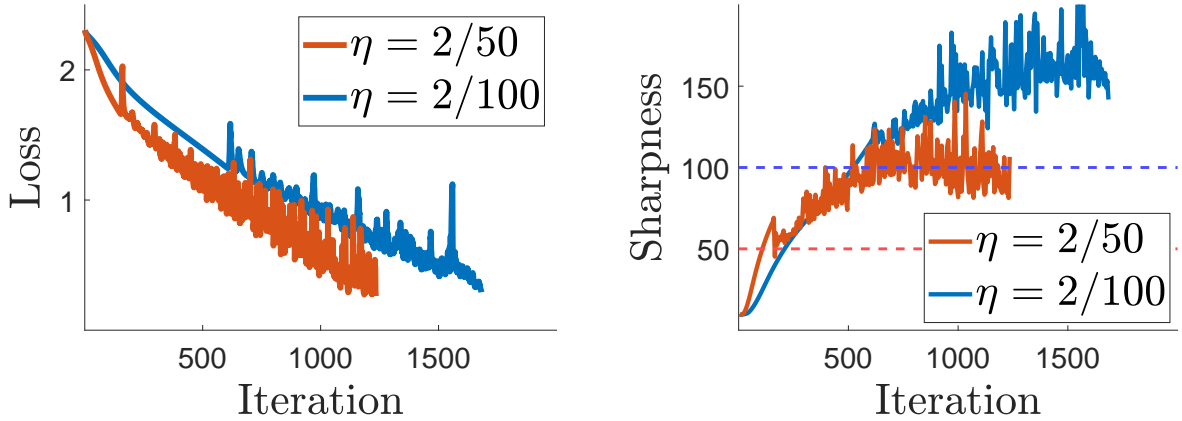


Figure 1: **Example of unstable convergence** for training CIFAR-10 with GD. We follow the experimental setup of Cohen et al. [2021]; see Experiment 1 for details. We use a ReLU network. Here, condition (2) fails, but the training loss still (non-monotonically) decreases in the long run.

Recently, it has been observed that GD on neural networks often violates condition (2). More specifically, Cohen et al. [2021] observe that when we run GD to train a neural network, the condition (2) fails, but contrary to the common wisdom from convex optimization, the training loss still (non-monotonically) decreases in the long run. See Figure 1 for an example of this phenomenon. We call this phenomenon **unstable convergence**.

Unfortunately, little is known about unstable convergence. The causes and implications of this phenomenon have not been explored in the literature. More importantly, the main features of this phenomenon have not been elucidated. Characterizing the main features is important because it not only furnishes better understanding, but also lays a foundation for future theoretical studies that are more aligned with practice.

Contributions. In light of the above motivation, the main contributions of this paper are as follows:

1. We explain the main causes driving the unstable convergence phenomenon (Section 3).
2. We identify the main features that characterize unstable convergence in terms of how loss, iterates, and sharpness¹ evolve with GD updates. Moreover, we investigate and clarify the relations between them. Our characterizations demonstrate that the features of unstable convergence are in stark contrast with those of traditional stable convergence, suggesting that their optimization mechanisms are significantly different.
3. We extend our discussion to the SGD setting.

Figure 2 provides a more technical overview of our contributions, as well as the intuition gained through them.

¹In this paper, following Cohen et al. [2021], sharpness means the maximum eigenvalue of the loss Hessian, i.e., $\lambda_{\max}(\nabla^2 f(\theta^t))$.

Unstable Convergence

What are its causes (Section 3):

- Lack of (flat) stationary points near GD trajectory
- Forward-invariance ($F(S) \subseteq S$) of the GD dynamics

What are its main features (Section 4):

Object	Quantity	Behavior
Loss (§4.1)	$RP(\theta^t)$	oscillates near 0
Iterates (§4.2)	$L(\theta^t; \eta \nabla f(\theta^t))$	oscillates near $2/\eta$
Sharpness (§4.4)	$\lambda_{\max}(\nabla^2 f(\theta^t))$	oscillates $\frac{\text{near}}{\text{above}} 2/\eta$

- **Relative Progress:** $RP(\theta) := \frac{f(\theta - \eta \nabla f(\theta)) - f(\theta)}{\eta \|\nabla f(\theta)\|^2}$
- **Directional smoothness:** $L(\theta; \mathbf{v}) := \frac{\langle \mathbf{v}, \nabla f(\theta) - \nabla f(\theta - \mathbf{v}) \rangle}{\|\mathbf{v}\|^2}$

- Loss behavior \Leftrightarrow Iterates behavior (Section 4.3)
- Loss behaviour \Rightarrow Sharpness behavior (Section 4.4)

Extension to SGD (Section 5)

Figure 2: Overview/summary of results.

1.1 Related work

Under various contexts, several recent works have observed the unstable convergence phenomenon in training neural networks with (S)GD [Wu et al. \[2018\]](#), [Xing et al. \[2018\]](#), [Lewkowycz et al. \[2020\]](#), [Jastrzkebski et al. \[2017, 2018\]](#). We refer readers to the related work section of [Cohen et al. \[2021\]](#) for greater context.

The unstable convergence phenomenon is first formally identified by [Cohen et al. \[2021\]](#), and in their paper it is named *edge of stability*. More specifically, they observe a more refined version of the unstable convergence: when training a neural network with GD, the sharpness at the iterate goes beyond the threshold $\eta/2$, and often saturates right at (or above) the threshold. Based on our discussion, in Section 5 we will explore the relations between our main features and their observed phenomenon.

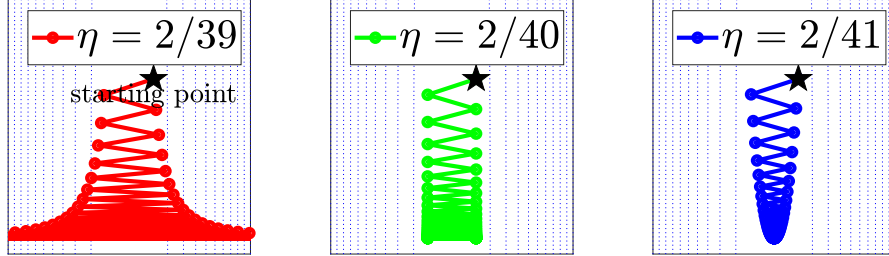
2 Warm-up: what does unstable regime suggest?

Empirically, unstable regime means that GD trajectory moves back and forth, and that the loss value oscillates. In this section, we would like to connect this description to mathematical quantities. In particular, we show that the fact that GD oscillates suggest that the smoothness constant is above the stable threshold and that the iterates are not at stationary points. We begin with the following well-known fact about the unstable regime in the case of quadratic costs.

Fact 1. On a quadratic cost $f(\boldsymbol{\theta}) = \frac{1}{2}\boldsymbol{\theta}^\top P\boldsymbol{\theta} + \mathbf{q}^\top \boldsymbol{\theta} + r$, then GD will diverge if any eigenvalue of P exceeds the threshold $2/\eta$. Moreover, for convex quadratics, this condition is “if and only if.” \square

Below we quickly illustrate this through an example.

Example 1. Consider optimizing a quadratic cost $f(\theta_1, \theta_2) = 20\theta_1^2 + \theta_2^2$. Note that in this case $L = 40$. Let us run GD on this cost with $\eta = 2/39, 2/40, 2/41$.



As shown in the above plots, GD converges to the optimum if $\eta < 2/L$ and it diverges if $\eta > 2/L$. \square

Due to the above fact, we often have the following intuition: if condition 2 is violated, then GD would diverge. Although this intuition is largely valid for convex optimization, it is not true in general. As a warm-up, we first discuss what the unstable regime actually suggests and develop some intuitions about the instability.

First, we show that GD cannot converge to a stationary point that has sharpness greater than $2/\eta$. We first make the following assumptions which says that the GD dynamics is nondegenerate and the spectrum of Hessian at stationary points is general.

Assumption 1. Let $F(\boldsymbol{\theta}) = \boldsymbol{\theta} - \eta \nabla f(\boldsymbol{\theta})$ and assume that for any subset S of measure zero, $F^{-1}(S)$ is of measure zero. Moreover, the subset $\{\mathbf{p} : \nabla f(\mathbf{p}) = 0, \frac{1}{\eta} \in \lambda(\nabla^2 f(\mathbf{p}))\}$ is of measure zero.

Theorem 1. For a given subset \mathcal{X} of the domain of variable $\boldsymbol{\theta}$, assume that f is C^2 in \mathcal{X} . Suppose that for each stationary point $\mathbf{p} \in \mathcal{X}$, it holds that either $\lambda_{\min}(\nabla^2 f(\mathbf{p})) < 0$ or $\lambda_{\max}(\nabla^2 f(\mathbf{p})) > \frac{2}{\eta}$. Then under Assumption 1, there is a measure-zero subset \mathcal{N} s.t. for all initializations $\boldsymbol{\theta}^0 \in \mathcal{X} \setminus \mathcal{N}$, the dynamics does not converge to any of the stationary points in \mathcal{X} .

Proof. See Appendix A. \square

Remark 1. Note that Theorem 1 applies to the case when the set of stationary points is not isolated.

The main takeaway of Theorem 1 is the following:

Takeaway 1. With probability one, GD cannot converge to stationary points even when they have a single sharp direction.

Given the above result, one might wonder if conversely, constant movement of GD is an “indicator” of GD being in the unstable regime. As a partial converse, we show that if the average of the squared gradient norm doesn’t decrease for a while, then GD is essentially in the unstable regime.

Proposition 1. Assume that $f \geq 0$. Suppose that for $\epsilon, \delta > 0$, there exists $K > \frac{f(\boldsymbol{\theta}^0)}{\eta\epsilon\delta}$ such that the last K tail average gradient norm is lower bounded by δ , i.e., $\frac{1}{K} \sum_{t=T}^{T+K-1} \|\nabla f(\boldsymbol{\theta}^t)\|^2 \geq \delta > 0$. Let L_t be the maximum sharpness between the iterates $\boldsymbol{\theta}^t$ and $\boldsymbol{\theta}^{t+1}$, i.e., $\max\{\lambda_{\max}(\nabla^2 f(\boldsymbol{\theta})) : \boldsymbol{\theta} \in \overline{\boldsymbol{\theta}^t \boldsymbol{\theta}^{t+1}}\}$. Then it follows that

$$\frac{\sum_{t=T}^{T+K-1} \|\nabla f(\boldsymbol{\theta}^t)\|^2 \cdot L_t}{\sum_{t=T}^{T+K-1} \|\nabla f(\boldsymbol{\theta}^t)\|^2} \geq \frac{2}{\eta} \cdot (1 - \epsilon).$$

Proof. See Appendix B. □

Thus far, we have discussed that being in the unstable regime suggests that GD is constantly moving. Having this intuition, we move on to understanding unstable convergence.

3 Causes for unstable convergence

It is expected that when the step size is too large for the smoothness level, the iterates will not converge. However, in practice we observe that under the unstable regime, GD can still “converge.” In this section, we study the cause for the co-occurrence for both behaviors.

3.1 What causes the unstable regime

In light of the discussion in Section 2, the unstable regime happens when GD is nonstationary. Here, we identify possible causes for the unstable regime in neural network training.

One possible cause for the unstable regime is that the landscape has only trivial stationary points (i.e., stationary points where all the weights are zero). This situation turns out to be very common for neural network models as illustrated by the following result.

Proposition 2. Assume the loss of neural network parametrized $\boldsymbol{\theta}$ contains a weight decay term as follows,

$$\ell(\boldsymbol{\theta}) = \frac{1}{n} \sum_{i=1}^n f(\mathbf{x}_i, \boldsymbol{\theta}) + \gamma \|\boldsymbol{\theta}\|_2^2.$$

If we partition the network parameter $\boldsymbol{\theta} = [\boldsymbol{\xi}; \boldsymbol{\zeta}]$ such that a subset of the network parameters $\boldsymbol{\zeta}$ is positive homogeneous, i.e. for any input data x_i and positive number $c > 0$

$$f(\mathbf{x}_i, [\boldsymbol{\xi}, \boldsymbol{\zeta}]) = f(x_i, [\boldsymbol{\xi}, c\boldsymbol{\zeta}]),$$

Then the loss $\ell(\boldsymbol{\theta})$ has no stationary point if $\boldsymbol{\zeta} \neq 0$.

Proof. This statement follows by a simple observation that from positive homogeneity,

$$\langle \nabla_{\boldsymbol{\zeta}} f(\mathbf{x}_i, [\boldsymbol{\xi}, \boldsymbol{\zeta}]), \boldsymbol{\zeta} \rangle = 0.$$

Therefore, if $\nabla_{\boldsymbol{\zeta}} \gamma \|\boldsymbol{\theta}\|_2^2 \neq 0$, we have

$$\nabla_{\boldsymbol{\zeta}} f(\mathbf{x}_i, [\boldsymbol{\xi}, \boldsymbol{\zeta}]) + \nabla_{\boldsymbol{\zeta}} \gamma \|\boldsymbol{\theta}\|_2^2 \neq 0,$$

which concludes the proof. □

Notice that the positive homogeneity parameters exist in many networks such as ResNet or Transformer when normalization layers exist ($\mathbf{a}_{L+1} = \mathbf{a}_L / \|\mathbf{a}_L\|$, where \mathbf{a}_L denote the input to layer L , and $\|\cdot\|$ denotes a norm of choice).

Another cause can be lack of flat minima near the GD trajectory. In the above example of ResNet or Transformer, the networks often add a small ϵ term to the normalization $\mathbf{a}_{L+1} = \mathbf{a}_L / (\epsilon + \|\mathbf{a}_L\|)$ to avoid the loss being undefined at $\mathbf{a}_L = 0$. However, the stationary points only exist when $\|\mathbf{a}_L\| \approx \epsilon$, in which case the sharpness of the stationary point is very large (on the order of $\sim 1/\epsilon$).

In fact, it has been extensively observed in the literature that the sharpness around GD with practical stepsize choices often goes beyond the threshold $2/\eta$. This claim is verified through a comprehensive set of experiments and called **progressive sharpening** in Cohen et al. [2021]; we refer readers to their Section 3.1 for details. For instance, the sharpness curve in Figure 1 shows this phenomenon. Moreover, a similar phenomenon was observed in Wu et al. [2018], and they speculated that the density of sharp minima is much larger than the density of flat minima in the neural network landscape. See their Section 4.1 for details.

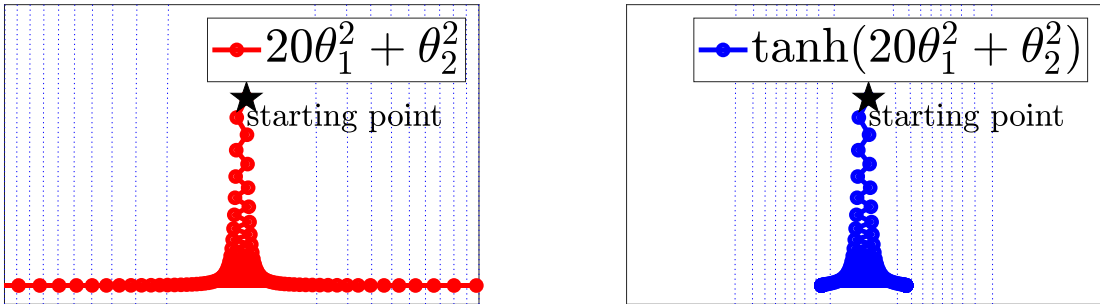
We summarize our discussion regarding the causes of unstable regime as follows.

Takeaway 2. *For practical stepsize choices, lack of (flat) non-trivial stationary points near the GD trajectory can cause GD to enter the unstable regime.*

3.2 Causes for convergence

As we discussed in Fact 1, for quadratic costs (or more generally for most convex optimization), GD being in the unstable regime implies that GD will diverge. However, as demonstrated by Cohen et al. [2021] through a comprehensive set of experiments, in neural network training, this situation no longer holds. In this section, we discuss how in the unstable regime “convergence” could happen through examples. As a warm-up, let us revisit the quadratic cost considered in Fact 1.

Example 2 (“Flattened” quadratic cost). *For the same quadratic cost as in Fact 1, we chose the same diverging step size $\eta = 2/39 > 2/L$, but this time we change the cost a bit by applying $\tanh(\cdot)$ on top of the quadratic cost. More formally, we consider the cost $\tanh(20\cdot\theta_1^2 + \theta_2^2)$. Due to the fact $\tanh \approx x$ near zero, this transformation wouldn’t change the geometry near the global minimum. We run GD on the two costs, and the results look as follows:*



As one can see from the above plot, for the transformed cost, GD does not diverge in the unstable regime. \square

The above toy example illustrates that indeed for nonconvex costs, being in the unstable regime does not necessarily mean divergence. For the above example, this was possible because of $\tanh(\cdot)$, which ‘flattens’ out the landscape of the quadratic cost away from the minimum.

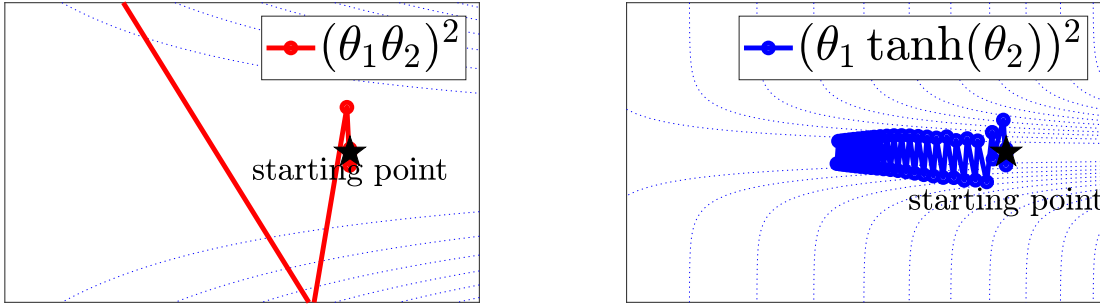
More formally, let us denote the GD dynamics by $F(\boldsymbol{\theta}) := \boldsymbol{\theta} - \eta \nabla f(\boldsymbol{\theta})$. Then the role of $\tanh(\cdot)$ in the above example is that it creates a compact subset near the minimum that is *forward-invariant*: we say S is forward-invariant with respect to the dynamics F if $F(S) \subseteq S$. Because the gradient of $\tanh(\text{quadratic})$ vanishes as the point gets farther away from the minimum, there exists a forward-invariant compact subset \mathcal{X} near the minimum.

We illustrate this point for neural network examples. We first consider the simplest neural network example, namely a single hidden neuron network.

Example 3 (Single neuron tanh network). *We consider a trivial task of fitting the data $(1, 0)$ with a single hidden neuron neural networks. Formally, we consider two types of networks:*

- *linear network*: $f(\theta_1, \theta_2) = (\theta_1 \cdot (1 \cdot \theta_2) - 0)^2$.
- *tanh network*: $f(\theta_1, \theta_2) = (\theta_1 \cdot \tanh(1 \cdot \theta_2) - 0)^2$.

We initialize both networks at $\boldsymbol{\theta}^0 = (13, 0.01)$ choose step size $\eta = 2/150$ to train them.

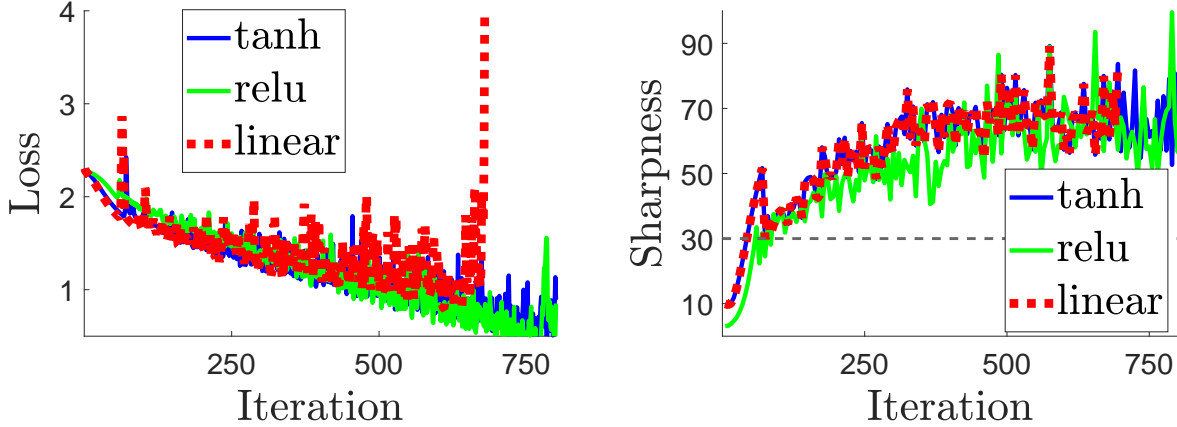


As one can see from the above plots, for a linear network, the iterate quickly diverges, while for the tanh network, the iterate does not diverge and converges to a minimum (whose sharpness is indeed approximately equal to $2/\eta$). \square

Example 3 illustrates that the use of activation function like \tanh can create a compact forward-invariant subset near the minima, which helps GD not diverge in the unstable regime. In fact, the above example suggests that GD indeed exhibits some convergence behaviour where while being in the unstable regime, GD travels along the valley of minima until it finds a flat enough minimum where it can stabilize.

We now consider more practical neural network examples inspired by the settings considered in Cohen et al. [2021].

Experiment 1 (CIFAR-10 experiment). *For this example, we follow the setting of the main experiment Cohen et al. [2021] in their Section 3, for which the unstable convergence is observed. Specifically, we use (full-batch) GD to train a neural network on 5,000 examples from CIFAR-10 with the CrossEntropy loss, and the network is a fully-connected architecture with two hidden layers of width 200. Under this common setting, we consider three types of networks: (i) linear network without activations; (ii) tanh activations; (ii) ReLU activations. We choose the step size $\eta = 2/30$ and the results are as follows:*



As one can see from the above plot, GD converges with the network activation functions in the unstable regime, but GD diverges without activation function. \square

We summarize our discussion regarding the cause of convergence as follows.

Takeaway 3. *Ingredients of a neural network such as activation functions create a compact forward-invariant set near the minima, which helps GD (non-monotonically) converge in the unstable regime.*

In this section, we have discussed the causes of unstable convergence and explain how the intuitions differ from those of conventional convex optimization. Another curious aspect of unstable convergence is the fact that the loss is very non-monotonic. We will explore the behavior of the loss in the next section.

4 Characteristics of unstable convergence

In this section, we aim to quantify unstable convergence through two computable quantities, the relative progress and the directional derivative. The first reflects the oscillation in loss, whereas the second reflects the oscillation in the iterates. We prove that these two quantities are closely related. We note that though smoothness breaks in neural network training, some other approximations in theoretical derivation can still lead to other valid assumptions.

4.1 Features in terms of loss behavior

We first investigate what happens to the loss under unstable convergence. As a warm-up, we first consider the loss behavior under **stable** convergence.

4.1.1 Warm-up: the stable regime

Recall from the descent lemma (1) that when GD is in the stable regime, then we have $f(\boldsymbol{\theta}^{t+1}) - f(\boldsymbol{\theta}^t) \leq -c\eta \|\nabla f(\boldsymbol{\theta}^t)\|^2$ for some constant $c > 0$. Putting it differently, we have

$$\frac{f(\boldsymbol{\theta}^{t+1}) - f(\boldsymbol{\theta}^t)}{\eta \|\nabla f(\boldsymbol{\theta}^t)\|^2} \leq -\text{const.}$$

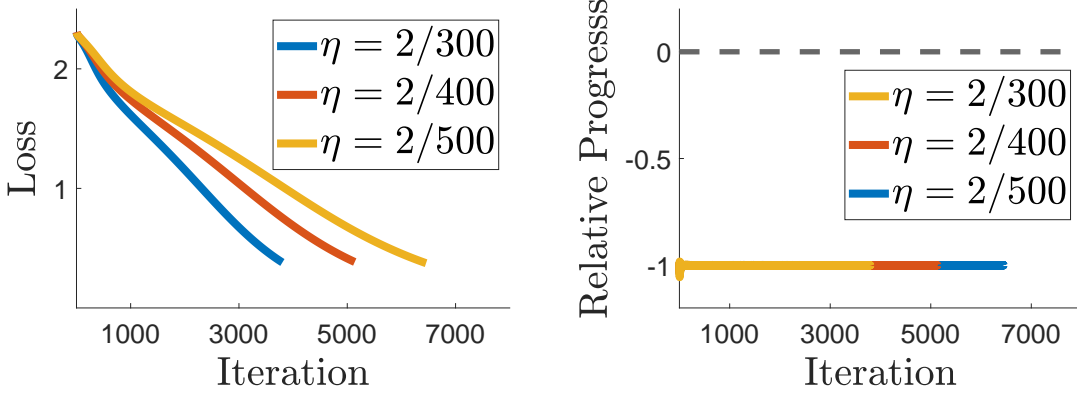
Let us give the ratio on the LHS a name:

Definition 1 (Relative progress ratio).

$$\text{RP}(\theta) := \frac{f(\theta - \eta \nabla f(\theta)) - f(\theta)}{\eta \|\nabla f(\theta)\|^2}.$$

Let us revisit Experiment 1 and verify that for smaller step sizes the relative progress ratio is indeed a negative number.

Experiment 2 (CIFAR-10; stable regime). *We use the same setting as Experiment 1, which follows the setting of the main experiment in Cohen et al. [2021]. For activations, we choose tanh following Cohen et al. [2021]. We choose much smaller step sizes so that GD is in the stable regime. We plot the loss and the relative progress ratio until the training accuracy hits 95%.*



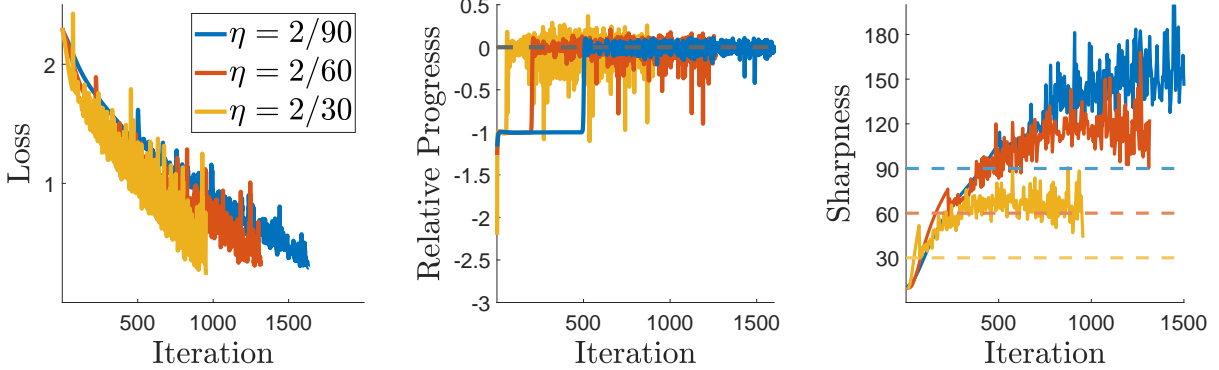
From the above plots, one can see that the relative progress ratio stays negative for all iterations. Moreover, there is no non-monotonic behavior in the loss curve. \square

Remark 2. Given the result above, one might wonder why the relative progress saturates around -1 . Although we do not have a clear explanation, we suspect that this happens because the trajectory of GD quickly converges to a single direction. We will quickly revisit this later this section. See Remark 5.

4.1.2 Relative progress under unstable convergence

Given that relative progress is strictly negative number in the stable regime, we now investigate how relative progress behaves in the case of unstable convergence.

Experiment 3 (CIFAR-10; unstable regime). *We use the same setting as Experiment 2, which follows the setting of the main experiment in Cohen et al. [2021], for which the unstable convergence is observed. This time we choose step sizes larger so that GD operates in the unstable regime. We plot the loss and the relative progress ratio until the training accuracy hits 95%.*



The above experiment shows that in the the unstable regime, the relative progress ratio saturates around 0 unlike the stable regime. \square

Remark 3. One noticeable aspect of the above plot is that the training seems to get faster as we choose larger step sizes. This is in fact one of the main observations in Cohen et al. [2021], suggesting that the unstable convergence is preferred in practice for its faster convergence. However, that does not mean one can increase the step size too large. For example, in the above experiment, we observe that the training loss diverge for step size $\eta = 2/8$.

Based on Experiment 3, we raise the following question:

Q. why does $\text{RP}(\boldsymbol{\theta}^t)$ oscillate around 0 under unstable convergence?

We begin with explaining why $\text{RP}(\boldsymbol{\theta}^t)$ cannot stay above 0. Since the loss is converging in a long term, it cannot be that $\text{RP}(\boldsymbol{\theta}^t) > 0$ for many iterations; otherwise, the loss will keep increasing, contradicting the convergence.

More curious part is the fact that $\text{RP}(\boldsymbol{\theta}^t)$ cannot stay below zero, which directly contrasts with the stable regime. To understand this phenomenon, we begin with some intuition.

We have seen that when GD encounters sharp minima, it oscillates near the minima as because it cannot stabilize to the minima (due to Theorem 1). In other words, the loss change $f(\boldsymbol{\theta}^{t+1}) - f(\boldsymbol{\theta}^t)$ would be much smaller compared to $\|\eta^2 \nabla f(\boldsymbol{\theta}^t)\|^2$ the square of the distance that GD travels. Hence, intuitively, one might expect that relative progress cannot be too negative under the unstable convergence. We would like to formalize this intuition.

4.2 Features in the iterates movement

To that end, let us formally define what it means for GD to oscillate. More generally, consider the situation where $\boldsymbol{\theta}$ is updated by moving along the vector $-\mathbf{v}$. Then this update is oscillatory if the directional derivative at the updated parameter $\boldsymbol{\theta} - \mathbf{v}$ is nearly negative of that at $\boldsymbol{\theta}$, i.e.,

$$\langle \mathbf{v}, \nabla f(\boldsymbol{\theta} - \mathbf{v}) \rangle \approx -\langle \mathbf{v}, \nabla f(\boldsymbol{\theta}) \rangle.$$

Inspired by this, we consider the following definition.

Definition 2 (Directional smoothness). *For an update vector \mathbf{v} , we define*

$$L(\boldsymbol{\theta}; \mathbf{v}) := \frac{1}{\|\mathbf{v}\|^2} \langle \mathbf{v}, \nabla f(\boldsymbol{\theta}) - \nabla f(\boldsymbol{\theta} - \mathbf{v}) \rangle.$$

Now coming back to the gradient descent where the update vector is $\mathbf{v} = \eta \nabla f(\boldsymbol{\theta})$, we have

$$L(\boldsymbol{\theta}; \eta \nabla f(\boldsymbol{\theta})) = \frac{\langle \nabla f(\boldsymbol{\theta}), \nabla f(\boldsymbol{\theta}) - \nabla f(\boldsymbol{\theta} - \eta \nabla f(\boldsymbol{\theta})) \rangle}{\eta \|\nabla f(\boldsymbol{\theta})\|^2}.$$

When GD is exhibiting oscillatory behaviour, we would have

$$\langle \nabla f(\boldsymbol{\theta}), \nabla f(\boldsymbol{\theta} - \mathbf{v}) \rangle \approx -\langle \nabla f(\boldsymbol{\theta}), \nabla f(\boldsymbol{\theta}) \rangle,$$

in which case, it holds that

$$L(\boldsymbol{\theta}; \eta \nabla f(\boldsymbol{\theta})) \approx \frac{2}{\eta} \quad \text{when GD iterates oscillate.} \quad (3)$$

For intuition, let us quickly verify (3) for quadratic costs.

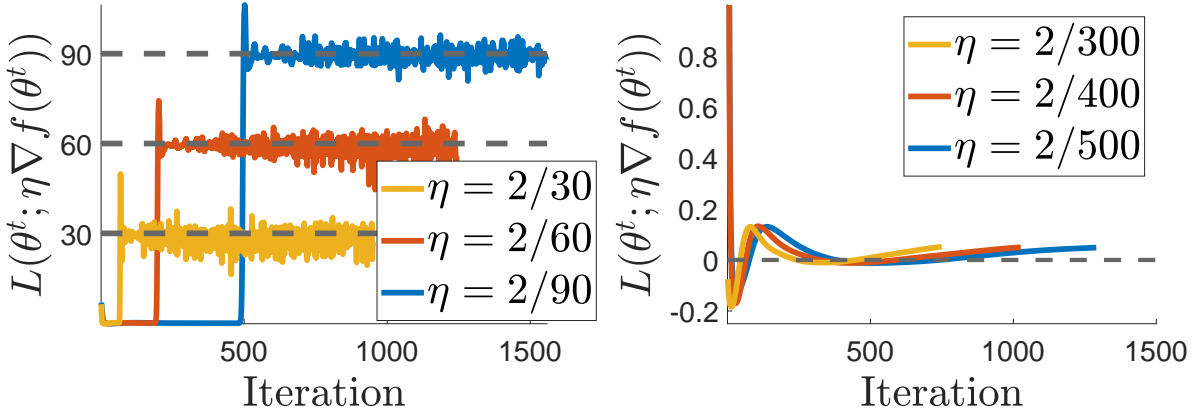
Example 4 (Quadratics). *Consider a quadratic loss function $f(\boldsymbol{\theta}) = \boldsymbol{\theta}^\top P \boldsymbol{\theta}$ with $P \succeq 0$. Then, the GD update reads $\boldsymbol{\theta}^{t+1} = (I - \eta P)\boldsymbol{\theta}^t$. For an eigenvector/eigenvalue pair (\mathbf{q}, λ) of P , the quantity $\langle \mathbf{q}_{\max}, \boldsymbol{\theta}^t \rangle$ evolves as*

$$\begin{aligned} \langle \mathbf{q}_{\max}, \boldsymbol{\theta}^t \rangle &= \mathbf{q}^\top (I - \eta P) \boldsymbol{\theta}^{t-1} = (1 - \eta \lambda) \langle \mathbf{q}_{\max}, \boldsymbol{\theta}^{t-1} \rangle \\ &= (1 - \eta \lambda)^t \langle \mathbf{q}_{\max}, \boldsymbol{\theta}^0 \rangle. \end{aligned}$$

This implies that if $\lambda < 2/\eta$, then $\mathbf{q}^\top \boldsymbol{\theta}^t \rightarrow 0$. Hence, if $\eta = 2/\lambda_{\max}(P)$, then after sufficiently large iterations t , we have $\boldsymbol{\theta}^t \approx (-1)^t \langle \mathbf{q}_{\max}, \boldsymbol{\theta}^0 \rangle \mathbf{q}_{\max}$, in which case $L(\boldsymbol{\theta}; \eta \nabla f(\boldsymbol{\theta})) \approx \frac{2}{\eta}$. \square

Given the above view on ‘‘oscillating’’ iterates, we now measure directional smoothness under unstable convergence.

Experiment 4 (Directional smoothness in stable and unstable regimes). *Under the same setting as Experiments 2 and 3, we measure the value $L(\boldsymbol{\theta}^t; \eta \nabla f(\boldsymbol{\theta}^t))$ at each iteration.*



Indeed, one can see that for the unstable regime $L(\boldsymbol{\theta}^t; \eta \nabla f(\boldsymbol{\theta}^t))$ saturates around $2/\eta$, indicating that GD is exhibiting an oscillating behavior. \square

Experiment 4 verifies that GD is indeed showing an oscillating behavior. We remark that a similar conclusion is made in [Xing et al. \[2018\]](#). Now coming back to our original question: *can we show a formal relation between the directional smoothness and the relative progress ratio?*

4.3 Relation between relative progress and direction smoothness

Theorem 2 formalizes our intuition that under the oscillating behavior of GD, $\text{RP}(\boldsymbol{\theta}^t)$ cannot stay below zero.

Theorem 2. *The following identity holds:*

$$\text{RP}(\theta) = -1 + \frac{\eta}{2} \cdot 2 \int_0^1 \tau \cdot L(\boldsymbol{\theta}; \eta\tau \nabla f(\boldsymbol{\theta})) \, d\tau. \quad (4)$$

Proof. See Appendix C. □

Theorem 2 implies that if the weighted average of $L(\boldsymbol{\theta}; \eta\tau \nabla f(\boldsymbol{\theta}))$ is close to $2/\eta$, namely

$$2 \int_0^1 \tau \cdot L(\boldsymbol{\theta}; \eta\tau \nabla f(\boldsymbol{\theta})) \, d\tau \approx \frac{2}{\eta},$$

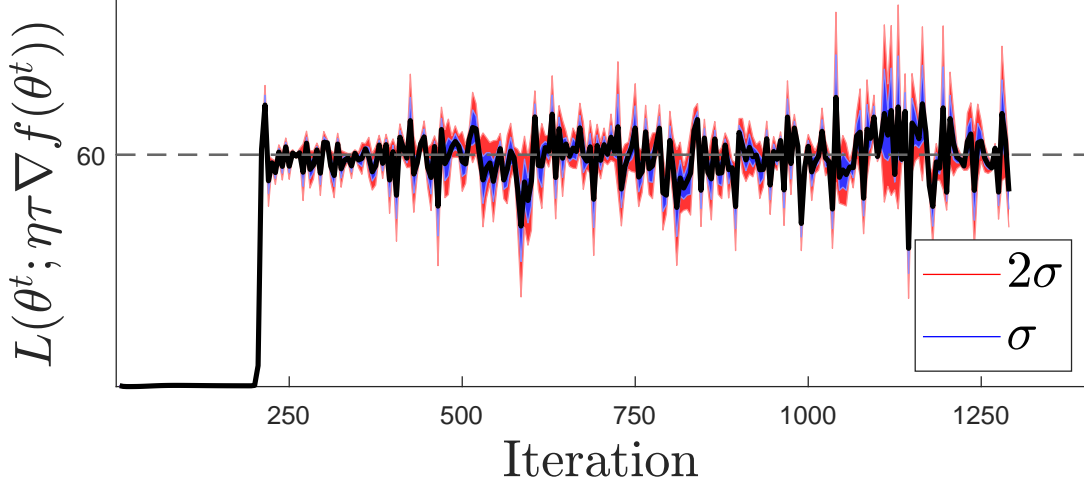
then $\text{RP}(\boldsymbol{\theta})$ is indeed approximately equal to zero. This formally justifies that when GD shows an oscillating behavior, $\text{RP}(\boldsymbol{\theta}^t)$ cannot stay below zero.

In our last experiment of this subsection, we verify that the above weighted average is approximately equal to the single value $L(\boldsymbol{\theta}; \eta \nabla f(\boldsymbol{\theta}))$, building a stronger relation between the directional smoothness and the relative progress ratio.

Experiment 5. *In the same setting as Experiment 3, we choose step size $\eta = 2/60$ and in every 5 iterations, we compute the following values:*

$$L(\boldsymbol{\theta}^t; \eta\tau \nabla f(\boldsymbol{\theta}^t)) \quad \text{for } \tau \in \{0.01, 0.02, \dots, 1\}.$$

In the plot below, we report the mean of $L(\boldsymbol{\theta}^t; \eta\tau \nabla f(\boldsymbol{\theta}^t))$ among $\tau \in \{0.01, 0.02, \dots, 1\}$ together with the shades which indicate the standard deviations.



This experiment verifies that $L(\boldsymbol{\theta}^t; \eta\tau \nabla f(\boldsymbol{\theta}^t))$ does vary much across $\tau \in [0, 1]$. □

Hence, Experiment 5 justifies the relation

$$\text{RP}(\theta) \approx -1 + \frac{\eta}{2} \cdot L(\boldsymbol{\theta}; \eta \nabla f(\boldsymbol{\theta})),$$

(5)

which precisely explains how the oscillatory behavior of GD results in a small relative progress.

Remark 4. The validity of equation (5) and Experiment 5 suggest that even though the gradient Lipschitzness is not a good assumption for neural networks, some form of Hessian Lipschitzness is valid along the GD trajectory.

We summarize the finding in this section as follows.

Takeaway 4. *Under the unstable convergence regime, $\text{RP}(\theta^t)$ oscillates near 0 for the following two reasons:*

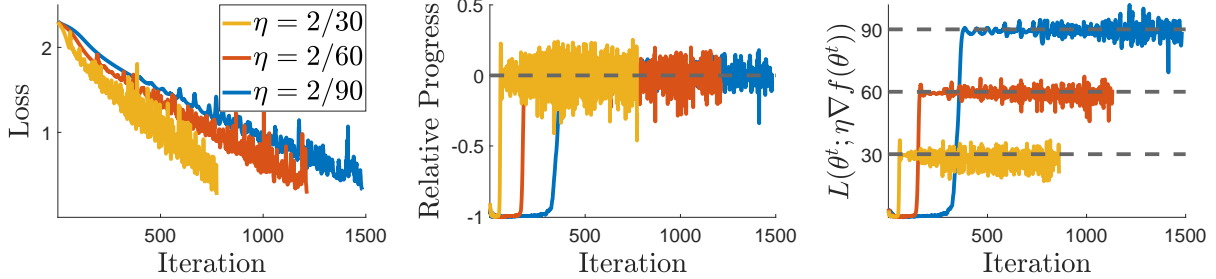
- $\text{RP}(\theta^t)$ can't stay above 0 because otherwise the loss would not decrease in the long run.
- $\text{RP}(\theta^t)$ can't stay below 0 due to the oscillating behavior of GD iterates. This is formalized via (5).

Remark 5. Given (5), one can have a clearer understanding on Remark 2 regarding why $\text{RP}(\theta^t)$ saturates around -1 . In the second result of Experiment 4, the directional smoothness remains very small in the stable regime. Based on (5), this implies that $\text{RP}(\theta^t)$ is close to -1 , which was indeed the case in Experiment 2.

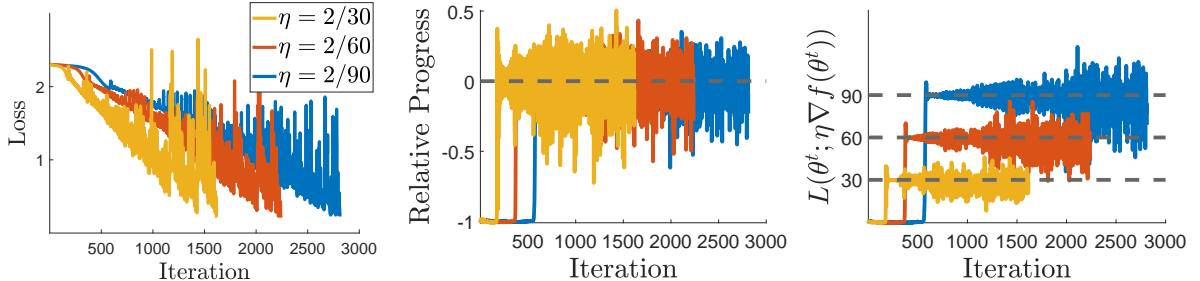
4.3.1 Additional experiments

In this subsection, we verify the relation (5) for other experimental settings.

Experiment 6 (CIFAR-10; ReLU networks). *Under the same setting as Experiment 2 (the setting of the main experiment in Cohen et al. [2021]), this time we choose ReLU as activation functions.*



In the next set of experiments, we put 2 more hidden layers of width 200 (total 4 hidden layers of width 200).



The results are largely similar to those for tanh activations, and the relation (5) holds for all cases. \square

4.4 Connection to sharpness and EoS

In this section, we investigate the implications of $\text{RP}(\theta^t)$ oscillating around 0. In particular, we discuss some relation to a curious phenomenon called *edge of stability* (EoS) recently observed in

Cohen et al. [2021]. The gist of their observation is that for GD on neural networks often satisfies the following properties: for $L(\boldsymbol{\theta}^t) := \lambda_{\max}(\nabla^2 f(\boldsymbol{\theta}^t))$,

- A. $L(\boldsymbol{\theta}^t) \geq 2/\eta$ for each iteration.
- B. In fact, in many cases $L(\boldsymbol{\theta}^t)$ saturates right at (or slight above) $2/\eta$.

To that end, we begin with the following consequence of Theorem 2.

Corollary 1. *Let L_t be the smoothness between the iterates $\boldsymbol{\theta}^t$ and $\boldsymbol{\theta}^{t+1}$, i.e., $\sup\{\lambda_{\max}(\nabla^2 f(\boldsymbol{\theta})) : \boldsymbol{\theta} \in \overline{\boldsymbol{\theta}^t \boldsymbol{\theta}^{t+1}}\}$. Then, the following inequality holds:*

$$\frac{2}{\eta} \cdot (\text{RP}(\boldsymbol{\theta}) + 1) \leq L_t.$$

Proof. It follows from the fact that for each $\tau \in [0, 1]$ $L(\boldsymbol{\theta}; \eta\tau \nabla f(\boldsymbol{\theta})) \leq \sup\{\lambda_{\max}(\nabla^2 f(\boldsymbol{\theta})) : \boldsymbol{\theta} \text{ lies on the line segment between } \boldsymbol{\theta}^t \text{ and } \boldsymbol{\theta}^t - \eta\tau \nabla f(\boldsymbol{\theta})\}$. \square

Corollary 1 implies that when $\text{RP}(\boldsymbol{\theta}^t)$ oscillates around 0, then L_t has to be frequently above the threshold $2/\eta$. One can actually refine this statement to understand the part A of EoS, given our results so far. In light of Experiment 5, if $L(\boldsymbol{\theta}^t; \eta\tau \nabla f(\boldsymbol{\theta}^t))$ does vary much across $\tau \in [0, 1]$, then one can actually write

$$\frac{2}{\eta} \cdot (\text{RP}(\boldsymbol{\theta}) + 1) \lesssim L(\boldsymbol{\theta}^t),$$

which is the part A of EoS.

Moreover, let us for a moment additionally assume that $\nabla f(\boldsymbol{\theta}^t)$ is approximately parallel to the largest eigenvector of the Hessian $\nabla^2 f(\boldsymbol{\theta}^t)$. This might look stringent at first glance, but given the calculations in Example 4, this assumption is true for unstable GD on a quadratic cost. Hence, it is possible that locally this condition is valid. Under this assumption, one can further deduce that

$$L(\boldsymbol{\theta}^t; \eta\tau \nabla f(\boldsymbol{\theta}^t)) \approx L(\boldsymbol{\theta}^t),$$

which together with Theorem 2 implies the part B of EoS.

5 Relative progress for SGD

In this section, we extend our discussion to the stochastic gradient descent (SGD):

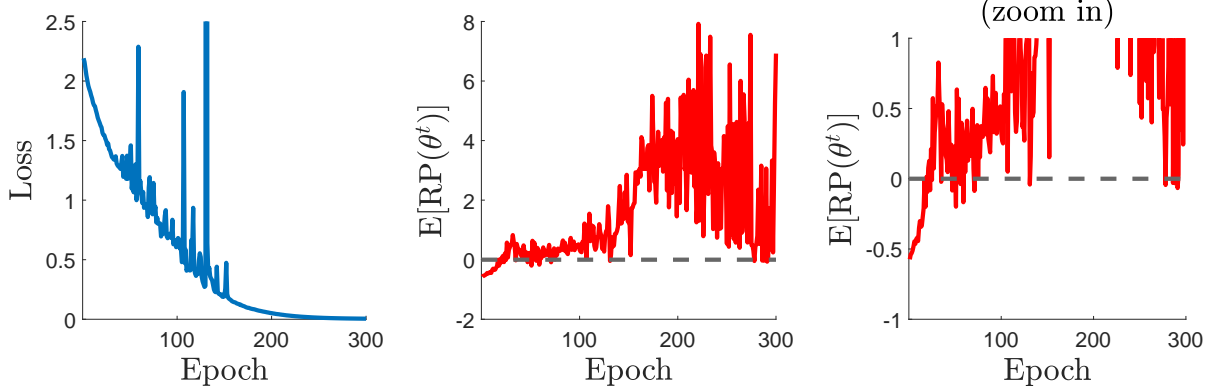
$$\boldsymbol{\theta}^{t+1} = \boldsymbol{\theta}^t - \eta g(\boldsymbol{\theta}^t), \quad \text{where } \mathbb{E}[g(\boldsymbol{\theta}^t)] = \nabla f(\boldsymbol{\theta}^t).$$

For the case of SGD, there is one obvious challenge. With SGD, the training loss does not decrease monotonically by nature since SGD is a random algorithm. Hence, it is not clear how to precisely define what it means for SGD to be in the unstable regime. On the other hand, inspired by our discussion in Section 4.1, a more transparent way to define the unstable regime for SGD is via the relative progress ratio. In particular, we consider the following extension to the SGD case.

Definition 3 (Expected relative progress ratio).

$$\mathbb{E}[\text{RP}(\boldsymbol{\theta})] := \frac{\mathbb{E}f(\boldsymbol{\theta} - \eta g(\boldsymbol{\theta})) - f(\boldsymbol{\theta})}{\eta \|\nabla f(\boldsymbol{\theta})\|^2}.$$

Experiment 7 (CIFAR-10; SGD on ReLU networks). *Under the same setting as Experiment 6, this time we train the network with SGD with minibatch size of 32 and step size $\eta = 2/100$. We compute the full-batch loss and the expected relative progress ratio at the end of each epoch.*



Note that $\mathbb{E}[\text{RP}(\theta^t)]$ does not stay below zero. Based on our discussion in Section 4.1, this suggests that SGD is in the unstable regime. \square

Remark 6. One very surprising aspect of the above results is that $\mathbb{E}[\text{RP}(\theta^t)]$ stays positive for majority of iterations. This seems to be contradicting the loss plot where SGD decreases the loss in the long run. However, we empirically verify that even when $\mathbb{E}f(\theta - \eta g(\theta)) - f(\theta)$ is positive, about 60% of minibatches give $f(\theta - \eta g(\theta)) - f(\theta) < 0$. In fact, this counter-intuitive phenomenon is also observed by Cohen et al. [2021] in a comprehensive set of experiments. See Section H therein for details.

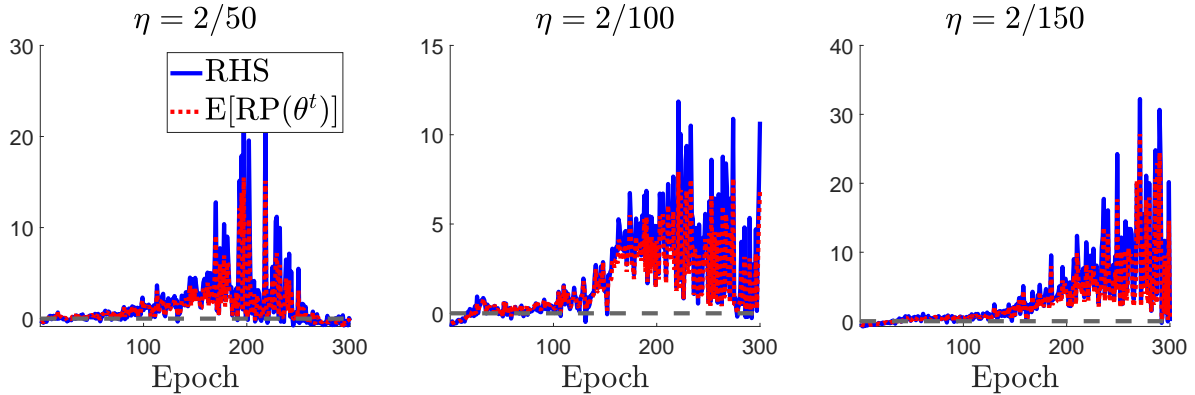
We now establish a relation analogous to (5) for SGD. Similarly to Theorem 2, one can prove the following equation:

$$\mathbb{E}[\text{RP}(\theta)] = -1 + \frac{\eta}{2} \cdot 2 \int_0^1 \tau \mathbb{E}_g \left[\frac{\|g(\theta)\|^2 \cdot L(\theta; \eta \tau g(\theta))}{\|\nabla f(\theta)\|^2} \right] d\tau.$$

See Appendix C for derivation. Hence, the analogous relation to (5) is:

$$\boxed{\mathbb{E}[\text{RP}(\theta)] \approx -1 + \frac{\eta}{2} \cdot \mathbb{E} \left[\frac{\|g(\theta)\|^2}{\|\nabla f(\theta)\|^2} L(\theta; \eta g(\theta)) \right].} \quad (6)$$

Experiment 8 (CIFAR-10; verifying (6)). *Under the same setting as Experiment 7, we compute $\mathbb{E}[\text{RP}(\theta)]$ and the RHS of (6) at the end of each epoch and compare those values. We choose step sizes $\eta = 2/50, 2/100, 2/150$.*



Note that the LHS and RHS of (6) are very similar in all results, verifying that the relation (6) holds for this case. We repeat this experiment for a tanh network, and the results can be found in Appendix D. \square

6 Discussion and future directions

This work demonstrated characteristics of unstable convergence that are in stark contrast with those of stable convergence. Consequently, this work leads to several interesting future directions.

- *Better optimizer?* The characteristics based on the directional smoothness suggests that the adjacent iterates have nearly opposite gradients in the unstable regime. This obviates the efficacy of many efficient methods (e.g. variance reduced methods) which are designed based on the intuition that the adjacent iterates have similar gradients. Hence, it would be interesting to design an efficient optimizer that respects the new characteristics.
- *Faster training under unstable convergence?* As discussed in Remark 3, another striking feature of unstable convergence is that the training loss seems to converge faster. One interesting question is whether one can elucidate this faster optimization by further exploring our characterization of relative progress.
- *What assumptions are valid for neural network optimization?* It is clear that unstable convergence cannot be reasoned with the widespread condition of $\eta < \frac{2}{L}$. Then what assumptions are valid for unstable convergence? For instance, as discussed in Remark 4, Experiment 5 suggests that although the gradient Lipschitzness is not a good assumption for neural networks, some form of Hessian Lipschitzness might be a valid one.
- *Unstable regime for adaptive methods?* Our characterizations are limited to constant step size (S)GD, and it is not clear how these characterizations carry over to adaptive methods such as Adam and RMSProp. Investigating adaptive methods will help us understand how they differ from (S)GD.

Acknowledgement

Suvrit Sra acknowledges support from an NSF CAREER grant (1846088), and NSF CCF-2112665 (TILOS AI Research Institute).

References

J. Cohen, S. Kaur, Y. Li, J. Z. Kolter, and A. Talwalkar. Gradient descent on neural networks typically occurs at the edge of stability. In *International Conference on Learning Representations*, 2021.

A. Jacot, F. Gabriel, and C. Hongler. Neural tangent kernel: convergence and generalization in neural networks. In *Proceedings of the 32nd Advances in Neural Information Processing Systems*, pages 8580–8589, 2018.

S. Jastrzkebski, Z. Kenton, D. Arpit, N. Ballas, A. Fischer, Y. Bengio, and A. Storkey. Three factors influencing minima in sgd. *arXiv preprint arXiv:1711.04623*, 2017.

S. Jastrzkebski, Z. Kenton, N. Ballas, A. Fischer, Y. Bengio, and A. Storkey. On the relation between the sharpest directions of dnn loss and the sgd step length. *arXiv preprint arXiv:1807.05031*, 2018.

J. Lee, L. Xiao, S. Schoenholz, Y. Bahri, R. Novak, J. Sohl-Dickstein, and J. Pennington. Wide neural networks of any depth evolve as linear models under gradient descent. *Advances in Neural Information Processing Systems*, 32:8572–8583, 2019.

J. D. Lee, M. Simchowitz, M. I. Jordan, and B. Recht. Gradient descent only converges to minimizers. In *Conference on learning theory*, pages 1246–1257. PMLR, 2016.

A. Lewkowycz, Y. Bahri, E. Dyer, J. Sohl-Dickstein, and G. Gur-Ari. The large learning rate phase of deep learning: the catapult mechanism. *arXiv preprint arXiv:2003.02218*, 2020.

Y. Li and Y. Liang. Learning overparameterized neural networks via stochastic gradient descent on structured data. In *Proceedings of the 32nd International Conference on Neural Information Processing Systems*, pages 8168–8177, 2018.

I. Panageas and G. Piliouras. Gradient descent only converges to minimizers: Non-isolated critical points and invariant regions. In *8th Innovations in Theoretical Computer Science Conference (ITCS 2017)*. Schloss Dagstuhl-Leibniz-Zentrum fuer Informatik, 2017.

M. Shub. *Global stability of dynamical systems*. Springer Science & Business Media, 2013.

L. Wu, C. Ma, et al. How SGD selects the global minima in over-parameterized learning: A dynamical stability perspective. *Advances in Neural Information Processing Systems*, 31:8279–8288, 2018.

C. Xing, D. Arpit, C. Tsirigotis, and Y. Bengio. A walk with sgd. *arXiv preprint arXiv:1802.08770*, 2018.

A Proof of Theorem 1

Proof. The proof is inspired by those of Lee et al. [2016], Panageas and Piliouras [2017]. First, we recall Stable Manifold theorem.

Theorem 3 (Stable manifold theorem Shub [2013] Thm III.7). *Let \mathbf{p} be a fixed point for the C^r local diffeomorphism $h : U \rightarrow \mathbb{R}^n$ where U is an open neighborhood of \mathbf{p} in \mathbb{R}^n and $r \geq 1$. Let $E^s \oplus E^c \oplus E^u$ be the invariant splitting of \mathbb{R}^n into the generalized eigenspaces of $Dh(\mathbf{p})$ corresponding to eigenvalues of absolute value less than one, equal to one, and greater than one. To the $Dh(\mathbf{p})$ -invariant subspace $E^s \oplus E^c$ there is an associated local h -invariant C^r embedded disc $W_{\text{loc}}^{s \oplus c}$ of dimension $\dim(E^s \oplus E^c)$ and ball B around \mathbf{p} such that*

$$h(W_{\text{loc}}^{s \oplus c}) \cap B \subset W_{\text{loc}}^{s \oplus c}. \quad \text{If } h^n(\mathbf{x}) \in B \text{ for all } n \geq 0, \text{ then } \mathbf{x} \in W_{\text{loc}}^{s \oplus c}. \quad (7)$$

Now we use Stable Manifold theorem to prove our main theorem. We first show that F is a local diffeomorphism around each stationary point \mathbf{p} . This follows from the inverse function theorem: (i) Note that F is a C^1 vector field since f is C^2 , (ii) the Jacobian of F is equal to $DF(\mathbf{p}) = I - \eta \nabla^2 f(\mathbf{p})$, and since $\frac{1}{\eta} \notin \lambda(\nabla^2 f(\mathbf{p}))$, the Jacobian is invertible. Hence, by inverse function theorem, we conclude that F is a local diffeomorphism around \mathbf{p} .

For each stationary point \mathbf{p} , we can thus apply [Theorem 3](#) at \mathbf{p} . Let $B_{\mathbf{p}}$ be the open ball due to [Theorem 3](#).

Then consider

$$\mathcal{C} = \bigcup_{\mathbf{p}: \text{stationary point}} B_{\mathbf{p}}$$

Since it is an open cover of \mathcal{C} , Lindelöf's lemma guarantees that there exists a countable subcover for \mathcal{C} , i.e., there exist $\mathbf{p}_1, \mathbf{p}_2, \dots$ s.t. $\mathcal{C} = \bigcup_{i=1}^{\infty} B_{\mathbf{p}_i}$. If GD converges to a stationary point \mathbf{p} , there must exist t_0 and i such that $F^t(\mathbf{p}_0) \in B_{\mathbf{p}_i}$ for all $t \geq t_0$. From [Theorem 3](#), we conclude that $F^t(\boldsymbol{\theta}_0) \in W_{\text{loc}}^{s \oplus c}(\mathbf{p}_i) \cap \mathcal{X}$ since $F(\mathcal{X}) \subset \mathcal{X}$. In other words, we have $\boldsymbol{\theta}_0 \in F^{-t}(W_{\text{loc}}^{s \oplus c}(\mathbf{p}_i) \cap \mathcal{X})$ for all $t \geq t_0$. Hence the set of initial points in \mathcal{X} for which GD converges to a stationary point is a subset of

$$\mathcal{N} := \bigcup_{i=1}^{\infty} \bigcup_{t=0}^{\infty} F^{-t}(W_{\text{loc}}^{s \oplus c}(\mathbf{p}_i) \cap \mathcal{X}).$$

Now from the assumption that either $\lambda_{\min}(\nabla^2 f(\mathbf{p})) < 0$ or $\lambda_{\max}(\nabla^2 f(\mathbf{p})) > \frac{2}{\eta}$, it follows that $I - \eta \nabla^2 f(\mathbf{p})$ has an eigenvalue whose absolute value is greater than 1. Hence, for each stationary point \mathbf{p} , $\dim(E^u) \geq 1$. This implies that each $W_{\text{loc}}^{s \oplus c}(\mathbf{p})$ has measure zero, and from the assumption that $F^{-1}(\mathcal{X})$ is of measure zero if \mathcal{X} is of measure zero, it holds that each $F^{-t}(W_{\text{loc}}^{s \oplus c}(\mathbf{p}_i) \cap \mathcal{X})$ is of measure zero. Thus, being a countable union of measure zero sets, \mathcal{N} is measure zero. It follows that for initialization $\boldsymbol{\theta}_0 \in \mathcal{X} \setminus \mathcal{N}$, the GD dynamics never approach \mathcal{C} , which implies that the limiting invariant measure doesn't contain \mathcal{C} in its support. This completes the proof. \square

B Proof of Proposition 1

For each t , the following inequality holds:

$$f(\boldsymbol{\theta}^{t+1}) - f(\boldsymbol{\theta}^t) \leq -\eta \|\nabla f(\boldsymbol{\theta}^t)\|^2 + \frac{\eta^2}{2} L_t \|\nabla f(\boldsymbol{\theta}^t)\|^2. \quad (8)$$

Summing (8) for $\boldsymbol{\theta} = \boldsymbol{\theta}^T, \boldsymbol{\theta}^{T+1}, \dots, \boldsymbol{\theta}^{T+K-1}$, we get

$$f(\boldsymbol{\theta}^T) - f(\boldsymbol{\theta}^0) \leq -\eta \sum_{t=T}^{T+K-1} \|\nabla f(\boldsymbol{\theta}^t)\|^2 + \frac{\eta^2}{2} \sum_{t=T}^{T+K-1} \|\nabla f(\boldsymbol{\theta}^t)\|^2 \cdot L_t. \quad (9)$$

Now suppose to the contrary that $L_t < (1 - \epsilon) \frac{2}{\eta}$ for all $t = T, \dots, T + K - 1$. Then, we have

$$-f(\boldsymbol{\theta}^0) \leq -\epsilon \eta \sum_{t=T}^{T+K-1} \|\nabla f(\boldsymbol{\theta}^t)\|^2 \leq -\epsilon \eta K \delta, \quad (10)$$

which is a contradiction.

C Proof of Theorem 2

Using the fact

$$\frac{d}{d\tau} [f(\boldsymbol{\theta} - \eta\tau \nabla f(\boldsymbol{\theta}))] = \langle -\eta \nabla f(\boldsymbol{\theta}), \nabla f(\boldsymbol{\theta} - \eta\tau \nabla f(\boldsymbol{\theta})) \rangle,$$

we obtain

$$\begin{aligned} f(\boldsymbol{\theta} - \eta \nabla f(\boldsymbol{\theta})) - f(\boldsymbol{\theta}) &= -\eta \int_0^1 \langle \nabla f(\boldsymbol{\theta}), \nabla f(\boldsymbol{\theta} - \eta\tau \nabla f(\boldsymbol{\theta})) \rangle d\tau \\ &= -\eta \|\nabla f(\boldsymbol{\theta})\|^2 - \eta \int_0^1 \langle \nabla f(\boldsymbol{\theta}), \nabla f(\boldsymbol{\theta} - \eta\tau \nabla f(\boldsymbol{\theta})) - \nabla f(\boldsymbol{\theta}) \rangle d\tau. \end{aligned}$$

Hence, after rearranging, we get

$$\frac{\eta}{2} \cdot 2 \int_0^1 \tau \cdot L(\boldsymbol{\theta}; \eta\tau \nabla f(\boldsymbol{\theta})) d\tau - 1 = \frac{f(\boldsymbol{\theta} - \eta \nabla f(\boldsymbol{\theta})) - f(\boldsymbol{\theta})}{\eta \cdot \|\nabla f(\boldsymbol{\theta})\|^2} = \text{RP}(\boldsymbol{\theta}),$$

which is precisely the relation in Theorem 2.

Derivation for the SGD case. For the SGD case, the derivation is similar.

$$\begin{aligned} f(\boldsymbol{\theta} - \eta g(\boldsymbol{\theta})) - f(\boldsymbol{\theta}) &\stackrel{(a)}{=} -\eta \int_0^1 \langle g(\boldsymbol{\theta}), \nabla f(\boldsymbol{\theta} - \eta\tau g(\boldsymbol{\theta})) \rangle d\tau \\ &= -\eta \langle g(\boldsymbol{\theta}), \nabla f(\boldsymbol{\theta}) \rangle - \eta \int_0^1 \langle g(\boldsymbol{\theta}), \nabla f(\boldsymbol{\theta} - \eta\tau g(\boldsymbol{\theta})) - \nabla f(\boldsymbol{\theta}) \rangle d\tau \end{aligned}$$

where (a) is due to the fact

$$\frac{d}{d\tau} [f(\boldsymbol{\theta} - \eta\tau g(\boldsymbol{\theta}))] = \langle -\eta g(\boldsymbol{\theta}), \nabla f(\boldsymbol{\theta} - \eta\tau g(\boldsymbol{\theta})) \rangle.$$

After taking expectation over the randomness in the stochastic gradient, we obtain

$$\mathbb{E} f(\boldsymbol{\theta} - \eta g(\boldsymbol{\theta})) - f(\boldsymbol{\theta}) = -\eta \|\nabla f(\boldsymbol{\theta})\|^2 - \eta \int_0^1 \mathbb{E} \langle g(\boldsymbol{\theta}), \nabla f(\boldsymbol{\theta} - \eta\tau g(\boldsymbol{\theta})) - \nabla f(\boldsymbol{\theta}) \rangle d\tau$$

Hence, after rearranging we obtain the desired equation:

$$\frac{\mathbb{E}f(\boldsymbol{\theta} - \eta g(\boldsymbol{\theta})) - f(\boldsymbol{\theta})}{\eta \|\nabla f(\boldsymbol{\theta})\|^2} = -1 + \frac{\eta}{2} \cdot 2 \int_0^1 \tau \cdot \mathbb{E}_g \left[\frac{\|g(\boldsymbol{\theta})\|^2 \cdot L(\boldsymbol{\theta}; \eta \tau g(\boldsymbol{\theta}))}{\|\nabla f(\boldsymbol{\theta})\|^2} \right] d\tau.$$

D Additional experiments for SGD

In this section, we repeat Experiment 8 with tanh activations. The results are similar to those of ReLu network as follows.

